

Flow simulation for P-Q curve analysis of fan impeller



B986040

Lee Han Jin

B986039

Lee Tae Hee

C086013

No Ho Yeong

C086029

Eom Tae Ung

C086011

Kim Ha Gyun

C186057

Kim Yu Bin

Table of Contents

1. Introduction

- 1.1 Operating Principle of Fan Impellers
- 1.2 Meaning and Principle of the P-Q Curve
 - 1.2.1 Meaning of the P-Q Curve
 - 1.2.2 Purpose of the P-Q Curve
- 1.3 Experimental Method for Obtaining the Fan's P-Q Curve
 - 1.3.1 Configuration of the Experimental Apparatus
 - 1.3.2 Measurement Procedure
 - 1.3.3 Specifications of the Experimental Apparatus and Measurement Locations
- 1.4 Target Fan Type and Geometry
- 1.5 Recent Technological Trends in CFD-Related CAE Tools

2. Fan Design and Geometry

- 2.1 CAD Model

3. Meshing Strategy

- 3.1 Mesh Condition Settings

4. Simulation Setting

4.1 Fluid Properties Required for Simulation

4.2 Boundary Conditions for Flow Analysis

5. Discussion

5.1 CFD Results Repeated at Fixed RPM Condition

(Table of Pressure and Flow Rate Values)

5.2 Comparison P-Q Curve Result

5.3 Comparison Between Simulation Results and Commercial Data Results

6. Conclusion

6.1 Professional Ethical Issues, Responsibilities, and Attitudes in Reporting CFD Results

6.2 Time and Cost Advantages of CFD-Based Analysis Methods

7. Reference

1. Introduction

1.1 Operating Principle of a Fan Impeller

A fan impeller generates flow by transferring kinetic energy to air or other fluids through rotating blades called "**impeller blades**."

The flow process consists of four stages.

1. Rotational Motion: The impeller rotates due to a motor. At this time, the peripheral speed **U** of the impeller is expressed as.

$$U = r \cdot \omega \quad r: \text{impeller radius}, \omega: \text{angular velocity}$$

2. Fluid Inflow: The rotating blades draw fluid either toward the central axis of the rotational radius or push it outward toward the periphery.

3. Kinetic Energy Transfer: The impeller transfers kinetic energy to the fluid, increasing its velocity.

The increase in specific energy imparted by the impeller can be expressed using Euler's Equation as:

$$\Delta h = U_2 V_{u2} - U_1 V_{u1}$$

Δh : energy per unit mass U : impeller peripheral speed

V_{u1} : tangential velocity components at the inlet, V_{u2} : tangential velocity components at the outlet

4. Pressure increase: As fluid velocity increases, static or total pressure also increases, generating flow.

The change in total pressure can be represented as

$$\Delta P_t = \Delta P_s + \frac{1}{2} \rho (V_2^2 - V_1^2)$$

ΔP_t : total pressure rise, ΔP_s : static pressure rise, V : fluid velocity, ρ : fluid density

1.2 Meaning and Applications of the P-Q Curve

1.2.1 Meaning of the P-Q Curve

The **P-Q curve** is a graphical representation of the performance of a **fan or pump**. It shows the **pressure** that a fan or pump can generate under various **volumetric flow rate** conditions. Typically, the x-axis represents the flow rate Q (volume flow rate), and the y-axis represents static pressure P.

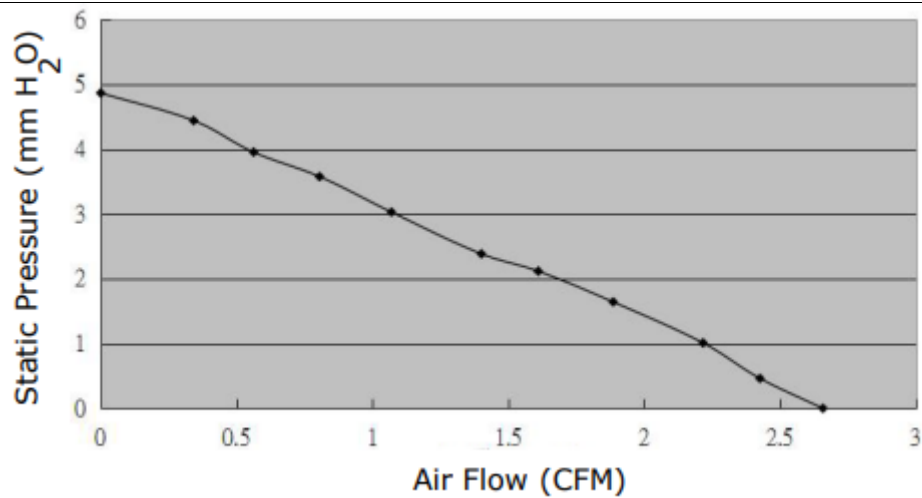
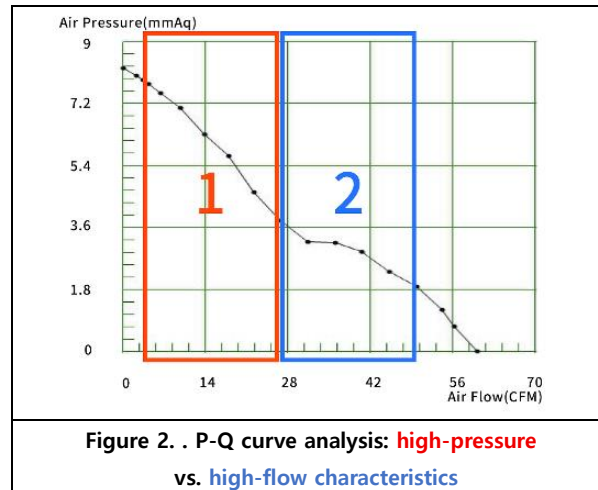


Figure 1. Performance graph (P-Q curve) of a blower fan

1.2.2 Applications of the P-Q Curve

1. Performance Evaluation of Fans and Pumps: The P-Q curve allows evaluation of how much pressure a fan can generate at a given flow rate.

By analyzing the shape of the curve, it is possible to determine whether a fan is optimized for high pressure or high flow rate. (fig 2.)

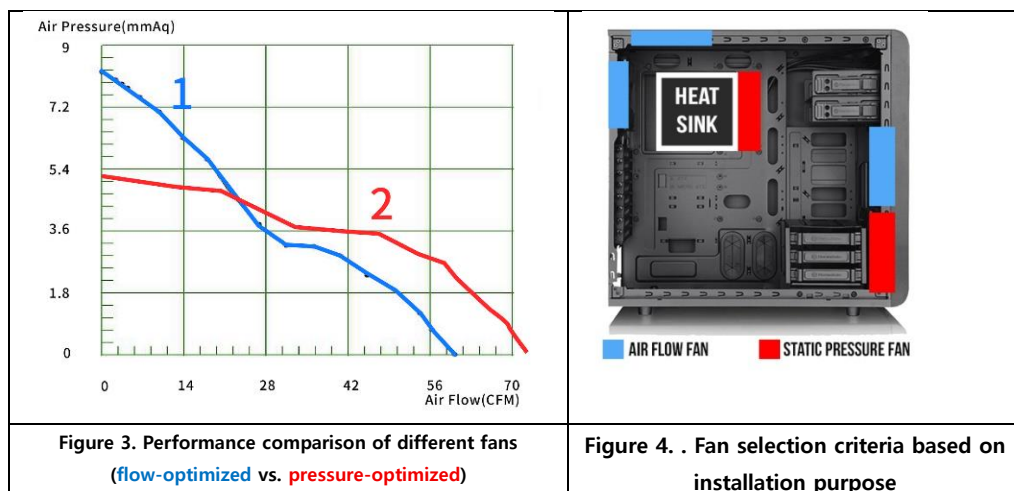


2. Selection of Appropriate Fan/Pump

By comparing the P-Q curves of various fans or pumps, the most suitable product for a specific application can be selected.

If the goal is to generate general airflow throughout an enclosed space, a fan with **high flow rate** is preferable.

If the goal is to create focused airflow in a high-resistance area like a computer heatsink or hard disk, a **high static pressure** fan is more suitable. (fig 3, fig 4)



3. Understanding Fan-System Interaction

By overlaying the system resistance curve onto the P-Q curve, the intersection point can be found, which is the operation point. This point predicts the actual operating condition of the fan. (fig 5)

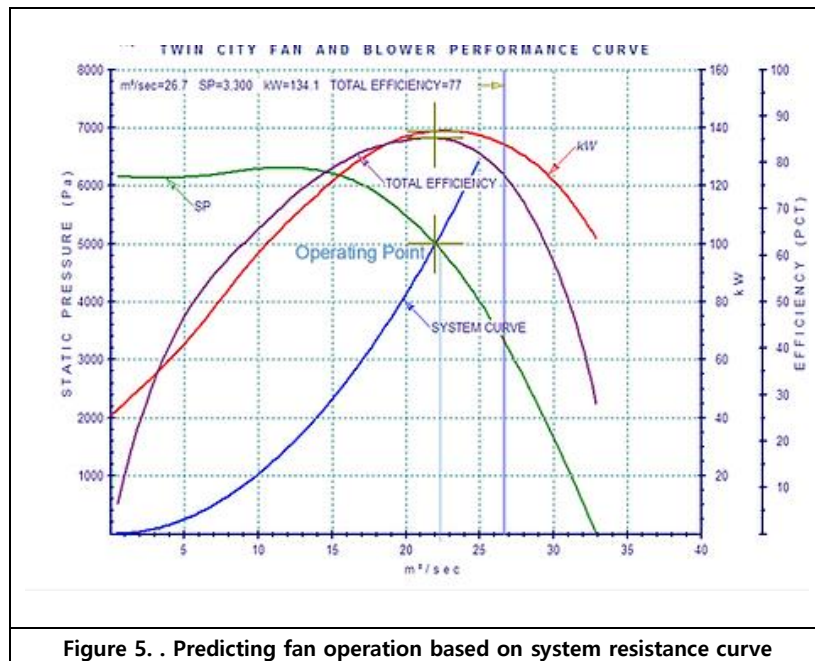


Figure 5. . Predicting fan operation based on system resistance curve

4. Analysis of Fan Operational Stability

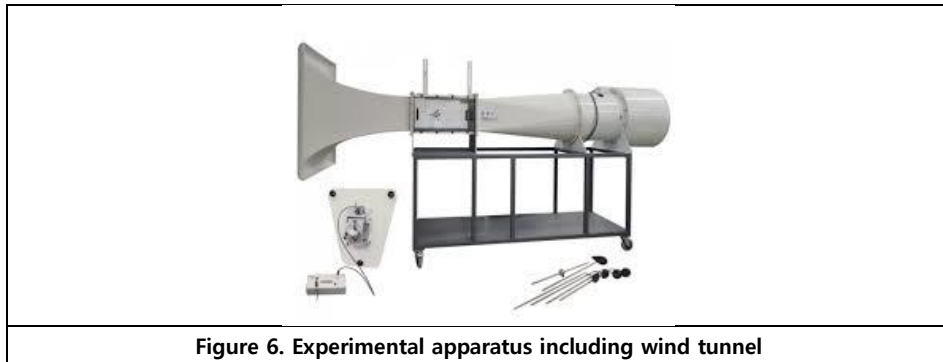
The P-Q curve helps determine the operational stability range of a fan.

It is possible to evaluate whether the fan can avoid unstable operations such as surge or stall

1.3 Experimental Method for Obtaining the P-Q Curve

1.3.1 Configuration of the Experimental Apparatus

Component	Description
Fan/Blower	The test subject to obtain the P-Q curve
Wind Tunnel or Duct System	Allows control and measurement of flow rate and pressure
Piezometer Ring, Static Tap	Measures static pressure inside the duct
Piezometer Ring, Pitot Tube	Measures dynamic pressure, mass flow rate, and volume flow rate
Damper or Outlet Regulator	Adjusts outlet area to create various flow conditions
RPM Meter	Maintains and records the rotational speed of the fan



1.3.2 Measurement Procedure

1. Initial Flow Rate Adjustment

Fully open the outlet to set the maximum flow condition.

2. Flow Condition Variation by Outlet Control

Gradually open or close the outlet using a damper or sliding plate.

3. Measurement

At each flow condition, repeatedly measure.

Static pressure, Volumetric flow rate (m^3/s or CFM)

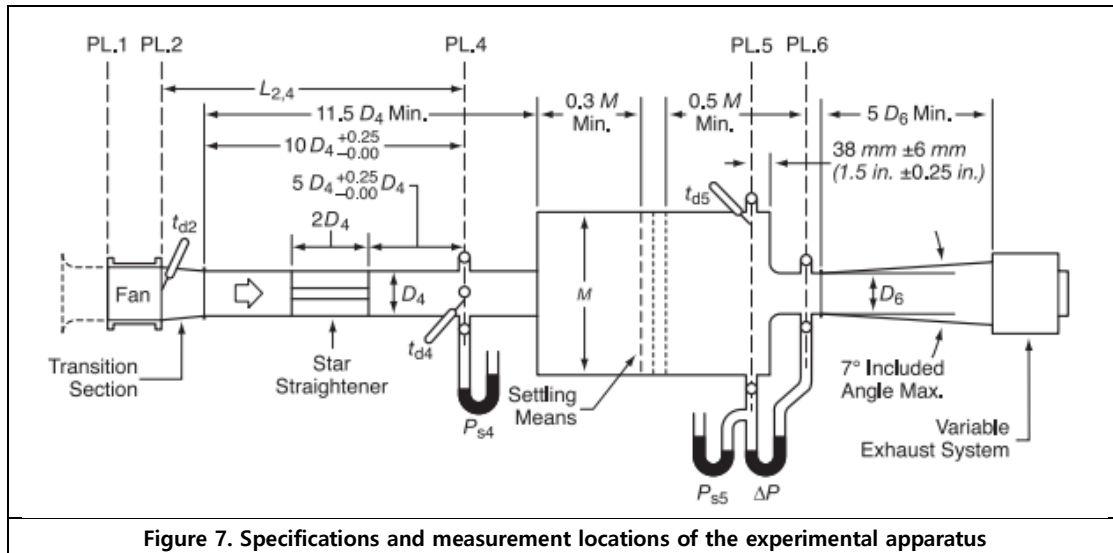
4. Data Processing and Graphing

X-axis: Flow rate (m^3/s or CFM), Y-axis: Pressure(Pa or mmH_2O)

1.3.3 Specifications and Measurement Locations of the Apparatus

(Based on AMCA 210 and ISO 5801 standards)

Item	Purpose/Target	Specification or Formula
Outlet Duct Diameter	D_4	$D_4 \geq 1.5D_{fan} \sim 2.0D_{fan}$
Equivalent Chamber Diameter	M	$M \geq 3D_4$
Measuring Duct Length (includes chamber, damper)	$L_{2,4} + 0.3M_{min} + 0.5M_{min}$	$L_{2,4} + 0.3M_{min} + 0.5M_{min} \geq 11.5D_4 + 0.9D_4 + 38(\text{mm}) + 1.5D_4$
Nozzle Diameter	D_6	$D_{6Max} = 0.53D_4$
Nozzle Angle	Angle_{Max}	$\text{Angle}_{Max} = 7^\circ$
Static Pressure Measurement Positions	PL. 4 PL. 5, PL. 6	$PL. 4 \geq 11.5D_4$ $PL. 5 \geq 12.4D_4$ $PL. 6 \geq 13.9D_4$
Flow Rate Measurement Position	$PL. 6$	$PL. 6 \geq 13.9D_4$
Measurement Equipment	measuring equipment	piezometer ring, static pressure taps



<Flow and Pressure formula>

$Q = Q_5 \left(\frac{\rho_5}{\rho} \right)$	$P_t = P_{t2} - P_{t1}$	$P_v = P_{v4} \left(\frac{A_4}{A_2} \right)^2 \cdot \left(\frac{\rho_4}{\rho_2} \right)$	$P_s = P_t - P_v$
$Q_5 = \sqrt{2C} A_6 Y \sqrt{\frac{\Delta P}{\rho_5}}$	$P_{t1} = 0$	$P_{v4} = \left(\frac{V_4}{\sqrt{2}} \right)^2 \cdot \rho_4$	$V_4 = \left(\frac{Q}{A_4} \right) \cdot \left(\frac{\rho}{\rho_4} \right)$
$P_{t2} = P_{s2} + P_{v4} + f \left(\frac{L_{2,4}}{D_n} - 2 \right) P_{v4} + 0.95(Re)^{-0.12} P_{v4}$			

<Test Data to be recorded>

Item Description	Parameter	Setup Figure
Barometric Pressure	P_b	○
Rotational Speed	N	○
Velocity Pressure	P_{v3r}	
Static Pressure	P_{s4}	○
Temperature	p_{s5}	○
	t_{d0}	○
	t_{w0}	○
	t_{d2}	○
	t_{d4}	○
	t_{d5}	○
Nozzle Pressure Drop	ΔP	○
Beam Load or Torque or Input Power	F or T or W	○

<Unit table>

Unit	Description	SI
CFM	Cubic Feet per Minute	$0.0004719 \text{ m}^3/\text{s}$
CMS	Cubic Meters per Second	$1 \text{ m}^3/\text{s}$
mmH₂O	Millimeters of Water Column	9.80665 Pa

< Classification and Description of Experimental Equipment >

Equipment Name	Description
Piezometer ring	A circular array of multiple static pressure taps evenly spaced around the inner circumference of a duct, used to measure average static pressure . Commonly used in fan testing for improved accuracy.
Static pressure tab	A single small hole or port on a duct wall that measures local static pressure perpendicular to flow. Simpler than a ring but less accurate for non-uniform flow
Pitot tube	A Pitot tube is a device used to measure fluid flow velocity by comparing total pressure and static pressure . It features two ports: one aligned with the flow to capture total pressure, and another positioned perpendicular to measure static pressure. The flow velocity is then calculated using Bernoulli's equation .
Damper	A damper is a mechanical device used in ducts or ventilation systems to control or regulate the flow of air or gas . It typically consists of adjustable blades or plates that can open, close, or modulate the airflow. Dampers are commonly used for balancing air distribution, isolating zones, or throttling flow in HVAC and industrial systems.
Chamber	A chamber is an enclosed section of a test setup or duct system used to stabilize airflow, simulate service conditions, or provide a controlled environment for pressure and flow measurements . Chambers may have circular or rectangular cross-sections and are often used in fan performance testing according to standards such as AMCA 210 or ISO 5801
Duct	A duct is a hollow conduit or channel used to transport air or other gases . Ducts are commonly used in HVAC systems (Heating, Ventilation, and Air Conditioning), industrial exhaust systems , wind tunnels , and other applications that involve airflow control and distribution.

1.3.4 Types of Fans

Fans are generally classified into **two major types**.

Fan Type	Max Flow Rate	Max Static Pressure	Flow Direct
Axial Fan	High	Low	Axial Direction
Centrifugal Fan	Moderate	High	Radial Direction

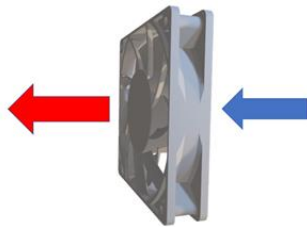


Figure 8 Shape and Flow Direction of an Axial Fan

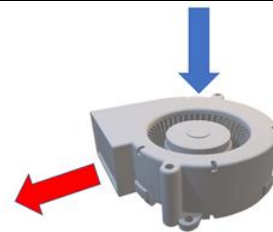


Figure 9 Shape and Flow Direction of a Centrifugal Fan

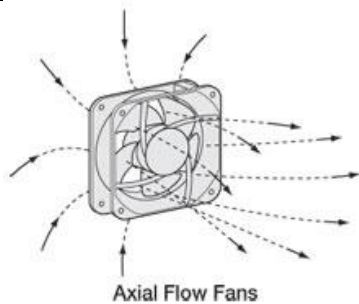


Figure 10. Airflow in an Axial Fan

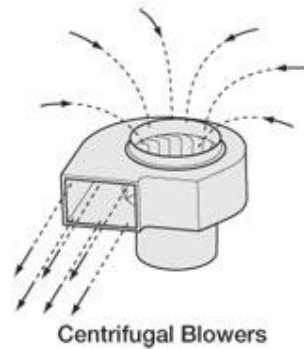
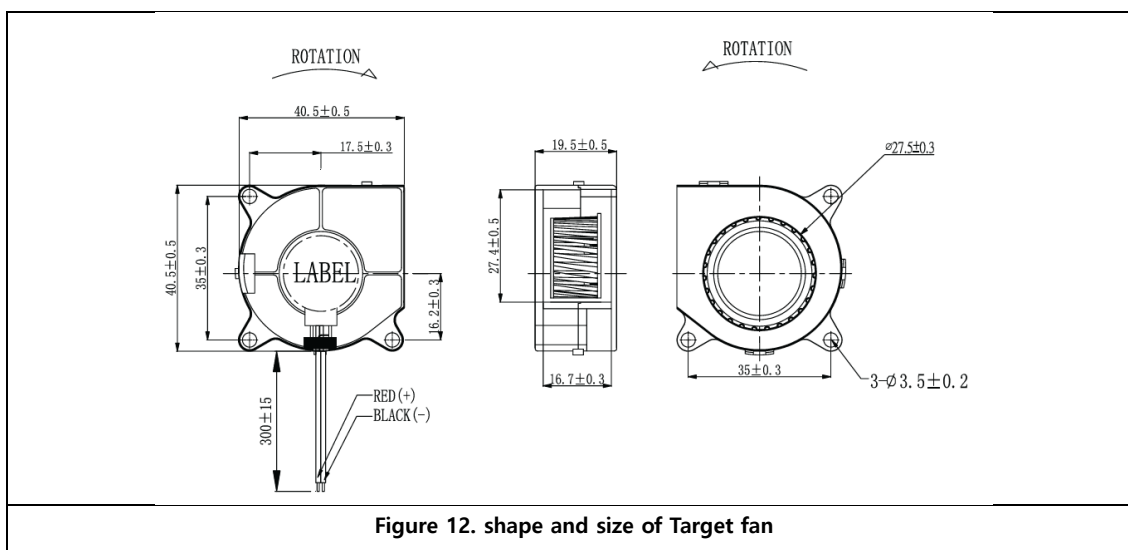


Figure 11. Airflow in a Centrifugal Fan

-> In this experiment, flow analysis is conducted using a **centrifugal-type fan**.

< Shape and Size of Target fan >

kind	Model name	size	inlet	Outlet	rpm
Centrifugal	CBM-4020B-160-367	40*40*20[mm ³]	ø27.5[mm]	27.4*16.4[mm ²]	6000



1.5 Recent Technological Trends in CFD-Related CAE Tools

In the field of CFD, the following innovative technologies have been rapidly advancing in recent years:

1. High-Resolution Mesh (Adaptive Mesh Refinement, AMR)

Major programs such as **ANSYS Fluent** offer **Adaptive Mesh Refinement (AMR)** functionality, which automatically refines or coarsens the mesh based on numerical analysis results. This enhances both computational efficiency and accuracy.

AMR focuses computational resources on regions where critical flow phenomena occur, while applying coarser meshes in less significant areas, thereby reducing overall computational load while maintaining precision.

2. Automated Optimization (Topology Optimization)

Recently, machine-learning-based techniques have enabled the optimization of mesh structures and geometries, allowing rapid creation of highly efficient analysis models even for complex fluid flows. For example, **MeshDQN** (Mesh Deep Q-Network) automatically optimizes CFD meshes using a reinforcement-learning approach (Deep Q-Network). By leveraging deep learning for mesh optimization, it lets users automatically generate more efficient grid structures even in intricate flow fields.

3. GPU Acceleration and Cloud Computing

Ansys was the first to adopt Omniverse Blueprint and applied it to its Ansys Fluent fluid simulation software, enabling accelerated CFD simulations.

Omniverse Blueprint is NVIDIA's industrial simulation framework that integrates GPU, AI, simulation tools, and digital twin technology into a single platform.

Using this technology, Ansys employed 320 NVIDIA GH200 Grace Hopper Superchips to complete a **2.5-billion-cell** automotive simulation in just over six hours—an analysis that would have previously taken nearly a month.

This breakthrough has significantly enhanced the feasibility of overnight high-fidelity CFD analysis and established a new industry benchmark.

4. AI-Based Turbulence Models & Digital Twins

Recent **learning-based subgrid-scale (SGS)** models using **AI** and **machine learning**—particularly in Large Eddy Simulation (LES) research—have demonstrated remarkable accuracy in uncertain flow regions. Reinforcement learning-based models have now achieved performance levels comparable to traditional LES approaches.

Traditional LES, a high-fidelity CFD technique for simulating turbulent flows, demands massive computational resources and has limitations due to its reliance on **SGS** models near boundary layers or in complex geometries. However, recent advances have improved these SGS models using reinforcement learning and deep learning techniques.

Integration with digital twins—virtual replicas that mirror real-world physical systems using live data—is also expanding rapidly. For example, by combining **NVIDIA Omniverse** with AI frameworks, real-time CFD-based digital twins can be implemented to monitor the performance of operational systems in real time and predict potential failures.

5. Multiphysics and Cloud Integration

(Centered on Altair, Siemens, and ANSYS)

Siemens has acquired Altair, leading to the enhancement of **AI-driven multiphysics** and **digital twin capabilities** within an integrated CFD platform, thereby expanding accessibility and usability of simulations.

ANSYS Cloud Direct, through integration with Microsoft Azure, enables immediate access to cloud-based HPC (High-Performance Computing), allowing large-scale simulations to be performed with ease.

As a result, shorter simulation times and more accurate reproduction of physical phenomena have made CFD an innovative and essential tool in R&D.

2. Fan Design and Geometry

2.1 CAD Model

The CAD model of the fan used for the simulation was based on the geometry of the **CBM-4020B-160-360-20** model from the manufacturer **[Same Sky]**.

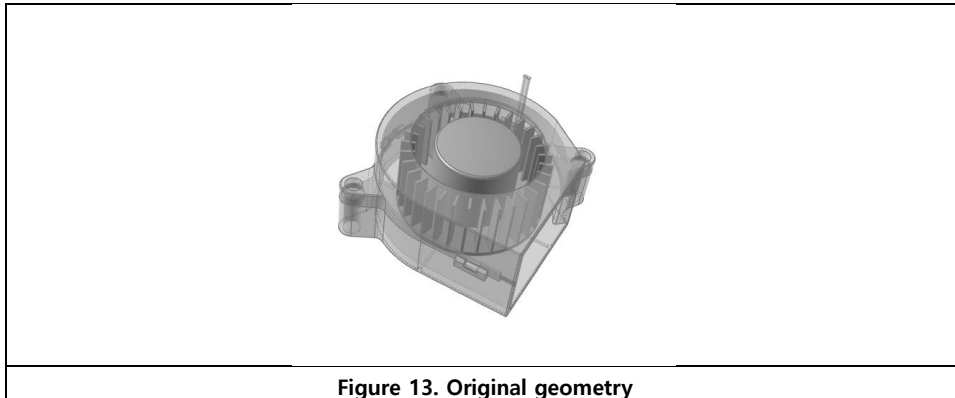
Since it was difficult to conduct CFD directly using the original geometry, the model was reconstructed using **Altair Inspire** software.

To cross-validate the accuracy of the results, fluid analysis was performed using both '**Altair SimLab**' and '**Ansys Fluent**' simulation software.

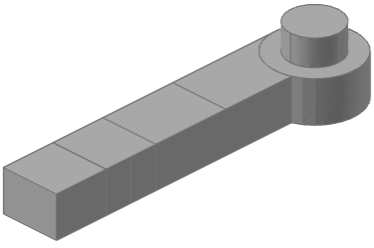
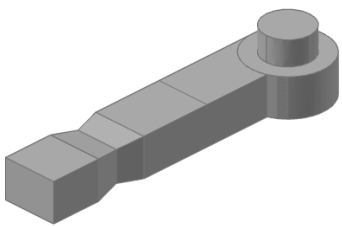
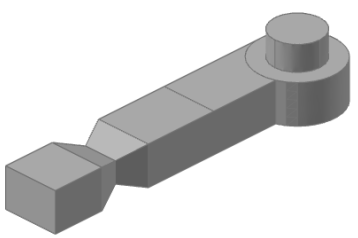
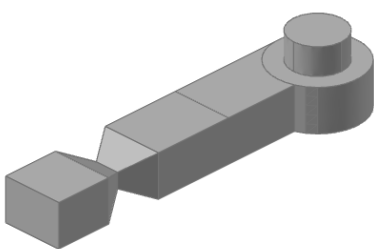
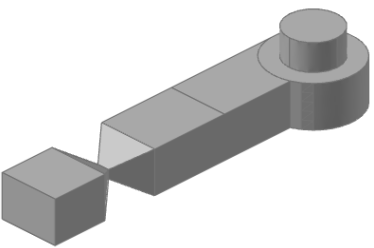
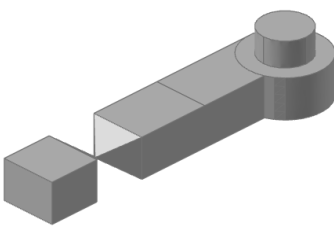
2.1.1. CAD Model for Simulation in SimLab

The geometry of the CAD model was constructed through the following process.

< Original Geometry >

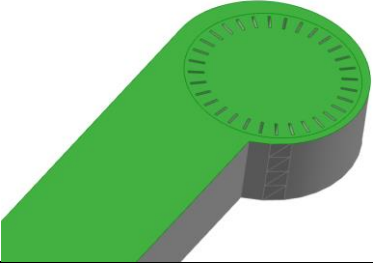
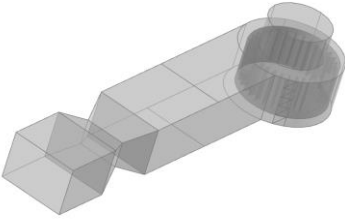


- Protrusions and cable structures of the model were removed, and a rectangular shape was added to the cylindrical body to simplify the geometry. (Figure 14)
- Protrusions and cable structures of the model were removed, and a rectangular shape was added to the cylindrical body to simplify the geometry. (Figure 14)
- All percentages refer to the outlet area.
(For example, 80% means that the outlet area is 80% of the original area.)

	
Figure 14. Optimized geometry at Area (100%)	Figure 15. Optimized geometry at Area (80%)
	
Figure 16. Optimized geometry at Area (60%)	Figure 17. Optimized geometry at Area (40%)
	
Figure 18. Optimized geometry at Area (20%)	Figure 19. Optimized geometry at Area (nearly 0%) Area = $0.5 * 0.5mm^2$

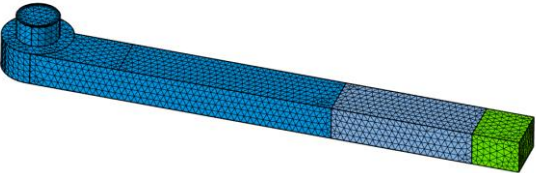
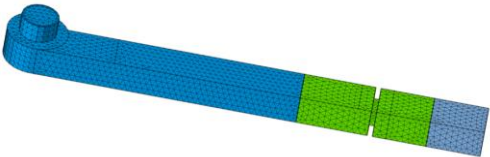

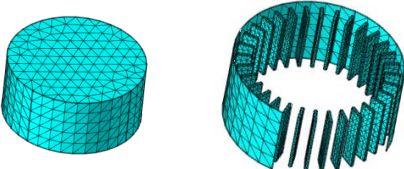
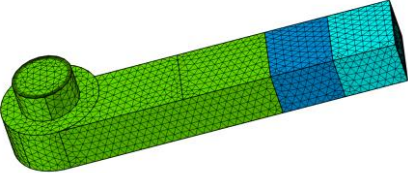
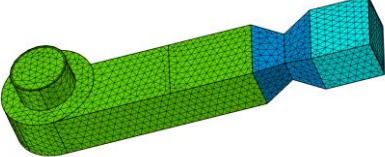
<Remodeling Only the Fluid Domain>

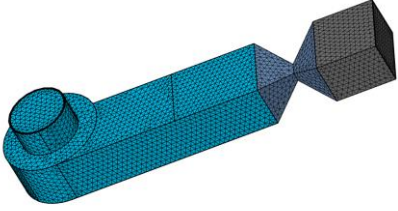
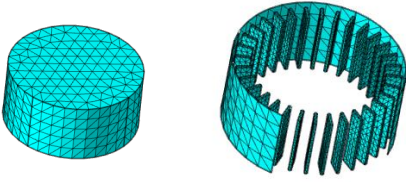
- Formed the **rotating region (Inner)** of the fan blades (Figure 20, 21)
- Conducted simulations while reducing the outlet area of the fan by **20% increments**.

	
<p>Figure 20. inlet Cross-Section</p>	<p>Figure 21. Rotating Region (Inner) Section</p>

<Preparation of Two Types of Models>

- **Type 1.** Duct length and damper shape similar to the actual experiment.
(Fig. 22, 23, 24, 25)
- **Type 2.** Shortened duct length and installed an inclined damper based on the previous model. (Fig. 26, 27, 28, 29)

	
<p>Figure 22. Optimized geometry at Area (100%)</p>	<p>Figure 23. Optimized geometry at Area (80%)</p>
	
<p>Figure 24. Optimized geometry at Area (0%)</p>	<p>Figure 25. Optimized geometry without axis</p>
	
<p>Figure 26. Optimized geometry at Area (100%)</p>	<p>Figure 27. Optimized geometry at Area (80%)</p>

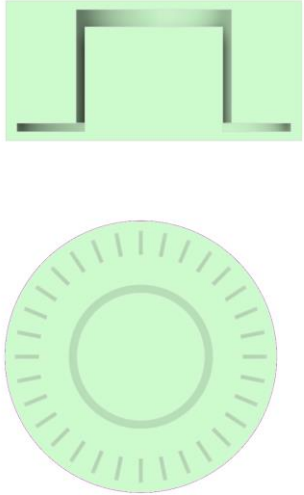
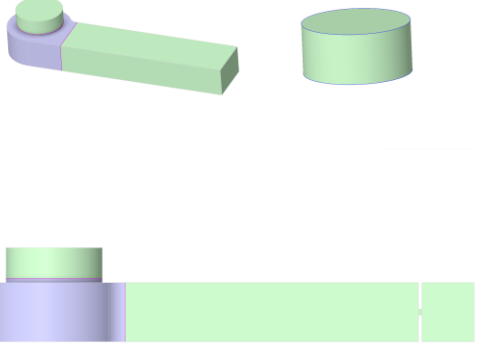
	
<p>Figure 28. Optimized geometry at Area (0%)</p>	<p>Figure 29. Optimized geometry without axis</p>

2.1.2 Geometry Used for Simulation in Ansys

In **Ansys Fluent**, the simulation was conducted without removing the hub located at the center of the fan blades to compare the results. (Figure 30)

As in **SimLab**, a cylindrical rotating region was separately defined around the fan blades. (Figure 30)

Similarly, the outlet area was reduced by 20% increments during the simulation. (Figure 21)

	
<p>Figure 30. Rotating Region Geometry</p>	<p>Figure 31. Overall Geometry of the Model for Simulation</p>

3. Meshing Strategy

3.1 Mesh Condition Settings

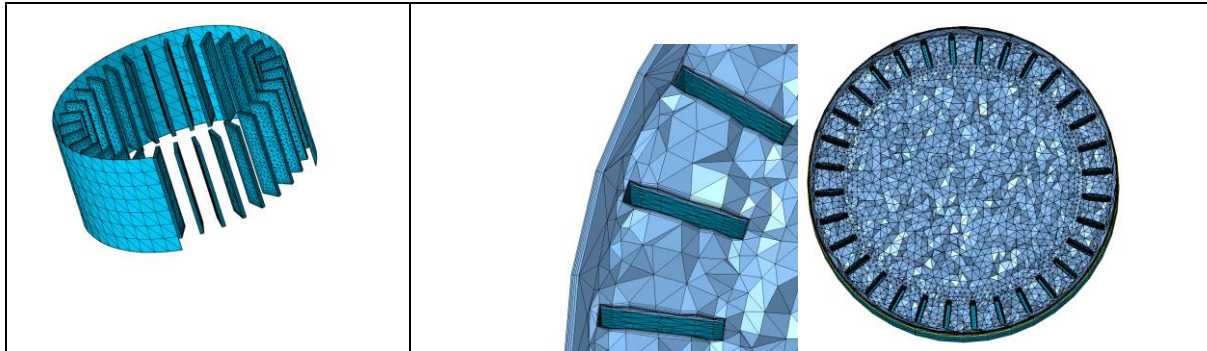


Figure 32. Mesh Conditions in the Rotating Region

The rotating region was set **more densely**.

The **number of layers** was set to **4** around the blade area and **5** in the rotating region.

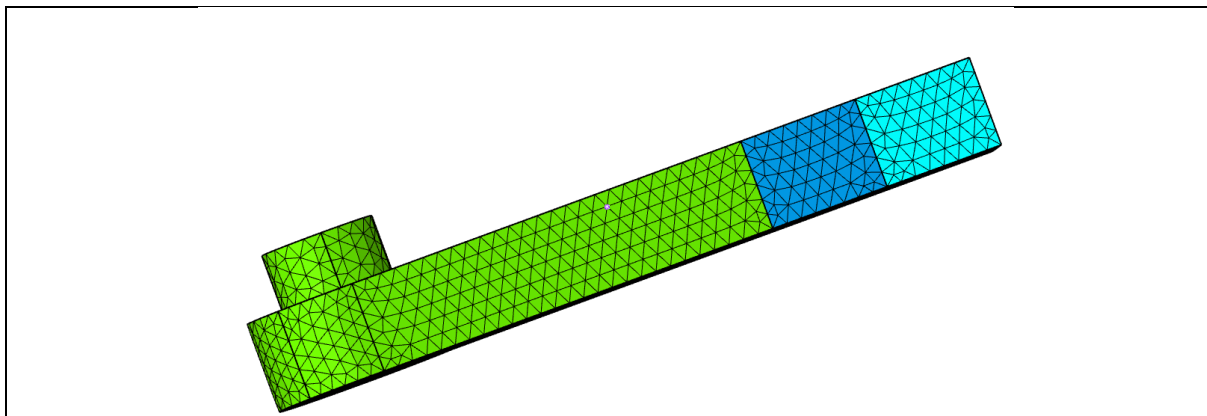


Figure 33. Surface Mesh In the Entire Duct

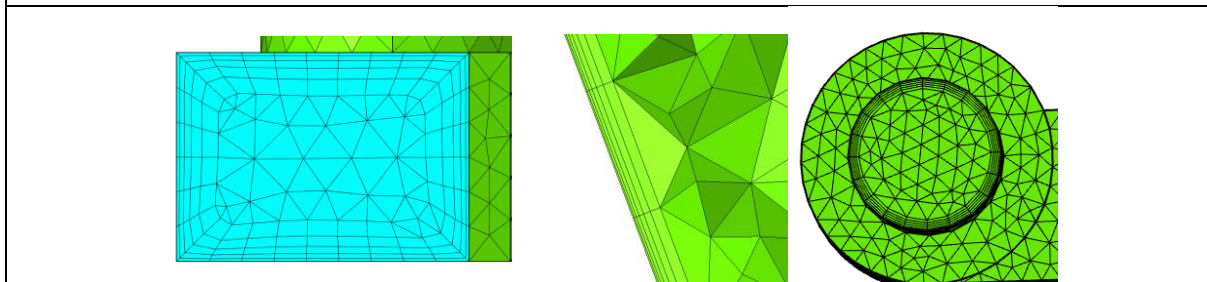


Figure 34. Surface Mesh in inlet, outlet, and wall surfaces

The **surface mesh** was set coarse, as it does not significantly affect the analysis.

The **inlet, outlet, and wall surfaces**, which are important for turbulence analysis, were set with **5 layers** for a denser mesh.

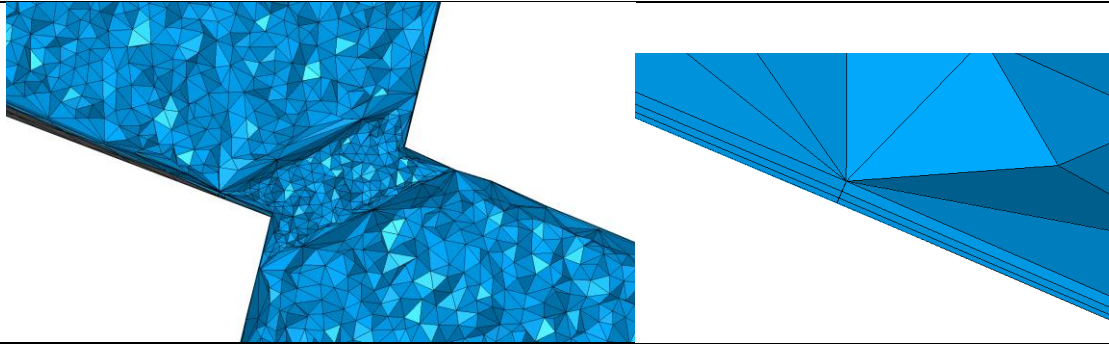


Figure 35. Mesh setting of narrowing section

The narrowing section of the damper, being a critical part of the analysis, was configured with a denser CFD mesh.

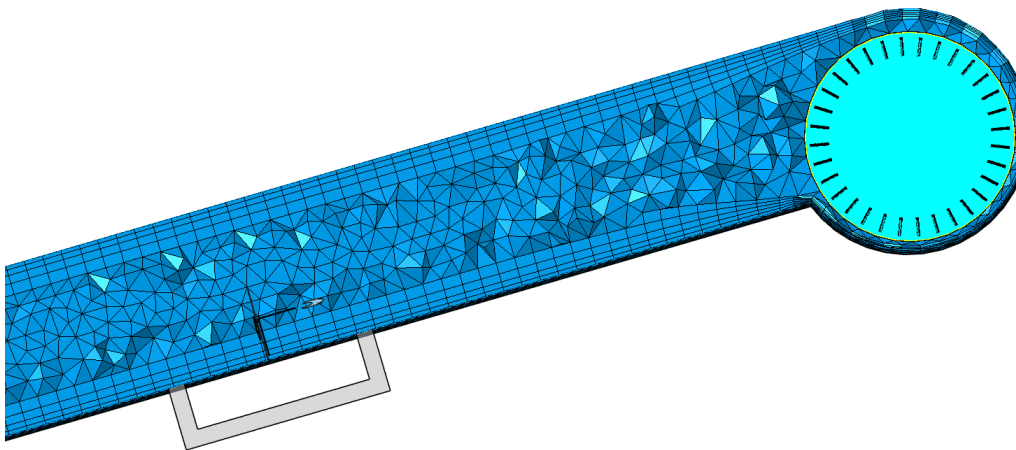


Figure 36. Mesh setting of non-critical regions

To reduce simulation time, the mesh was deliberately set coarser in non-critical regions.

4. Simulation Setting

4.1 Fluid Properties Required for Simulation

The diameter and height of the fan are 40 [mm] and 20 [mm], respectively, and the rotational speed for CFD analysis is set to $\omega = 6000$ [RPM].

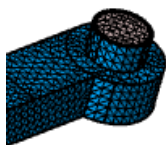
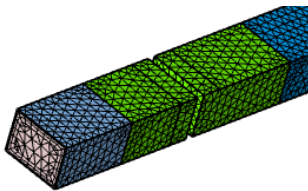
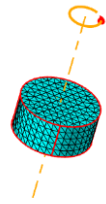
The working fluid passing through the fan was defined as '**Air**' to reflect the actual operating conditions. Properties such as the density and viscosity of air were assigned based on the built-in database provided in **SimLab**.

Database of 'Air'			
Name			value
Fluid Properties	Density	Type	Constant
		Density	1.225k/m ³
		Isothermal Compressibility	0.0
	Specific Heat		1005 J(kg*K _o)
	Latent Heat Effect		None
	Viscosity	Type	Constant
		Viscosity	1.781e-05 N*s/m ²
	Conductivity	Type	Constant
		Conductivity	0.02521 W(m*K)
	Radiation	Radiation Effect	FALSE
Magnetic Properties		Type	Soft Magnetic
		BH-Curve	Linear
		Relative permeability	1
Electrical Properties		Electrical resistivity	1.3e16 Ohm*m

4.2 Boundary Conditions for Flow Analysis

In SimLab, **three types of boundary conditions** were defined:

inlet, outlet, and reference frame.

inlet		outlet		Reference frame	
Inflow type	Stagnation Pressure 0[Pa]	Static Pressure	0[Pa]	angular velocity	630[rad/s]≅6000[RPM]
Hydrostatic Pressure	None	Hydrostatic Pressure	None	Centrifugal force	Yes
Turbulence input type	Auto	Back flow condition	None	Coriolis force	Yes
Turbulence flow type	Internal	Pressure loss factor	0	Angular acceleration force	Yes
Turbulence viscosity ratio	40	Integrated time step frequency	1		
Integrated output frequency	1	Statistics output frequency	0	Multiplier function	Yes
Satatic output frequency	1				
Nodal output frequency	0	Nodal output frequency	0	Axis of rotation	Straight/Arc edge: Counterclockwise (CCW)
Number of saved states	0	Number of saved states	0		
					
Figure 37. Inlet geometry			Figure 38. Outlet geometry		Figure 39. Reference frame geometry

5. Discussion

5.1 CFD Results Repeated at Fixed RPM Condition

(RPM Setting: Fixed at 6000 RPM)

5.1.1 Ansys Model

Opening Rate	Pressure Difference (Pa)	Mass Flow Rate (kg/s)	Volumetric Flow Rate (m ³ /s)
100%	0.1030671	0.00148349	0.00121101
80%	3.0060254	0.00140312	0.00114541
60%	7.4048749	0.00125979	0.0010284
40%	13.964027	0.00095943	0.00078321
25%	22.359361	0.00064749	0.00052856
20%	23.038373	0.00055123	0.00044999
10%	28.716405	0.00028004	0.0002286
5%	30.915639	0.00014657	0.00011965
1%	33.195163	2.88E-05	2.3522E-05

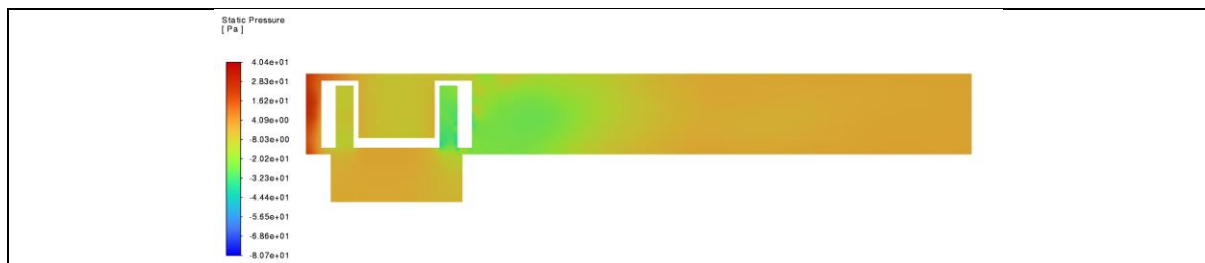


Figure 40. Static Pressure at Area (100%)

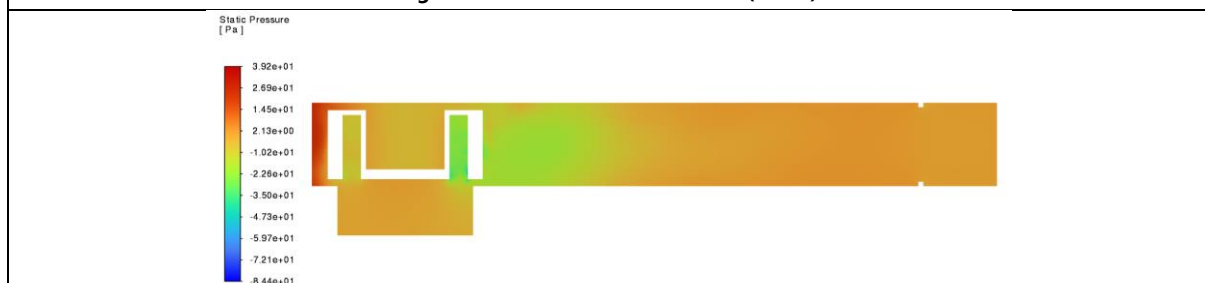


Figure 41. Static Pressure at Area (80%)

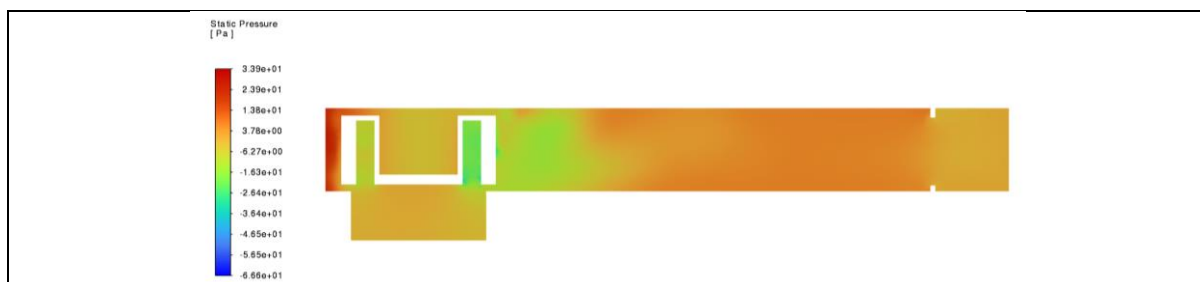


Figure 42. Static Pressure at Area (60%)

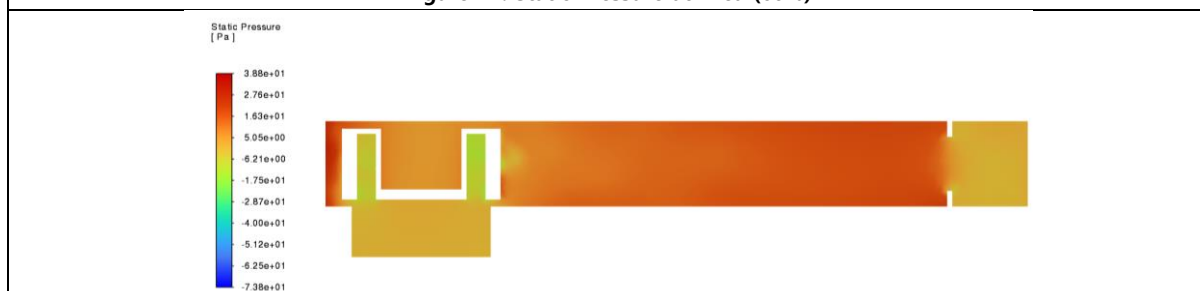


Figure 43. Static Pressure at Area (40%)



Figure 44. Static Pressure at Area (25%)

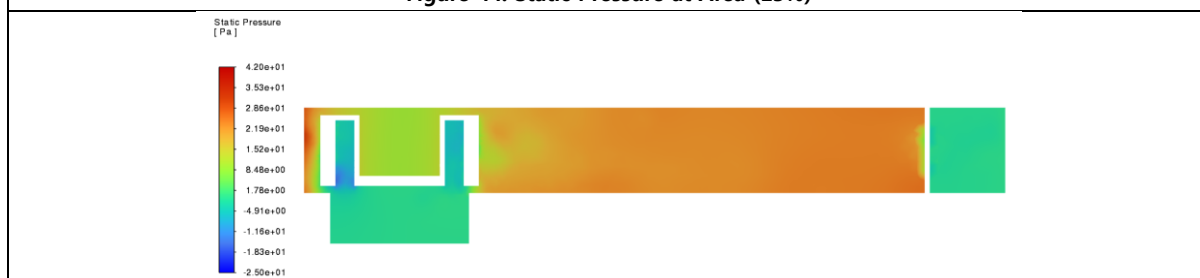


Figure 45. Static Pressure at Area (20%)

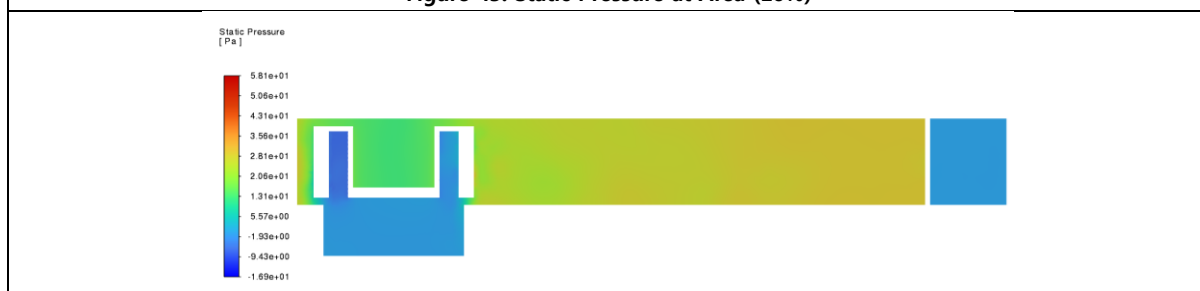


Figure 46. Static Pressure at Area (10%)

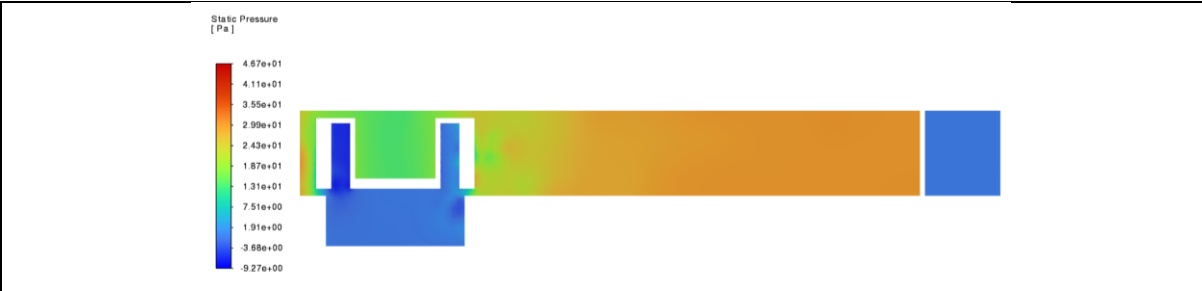


Figure 47. Static Pressure at Area (5%)

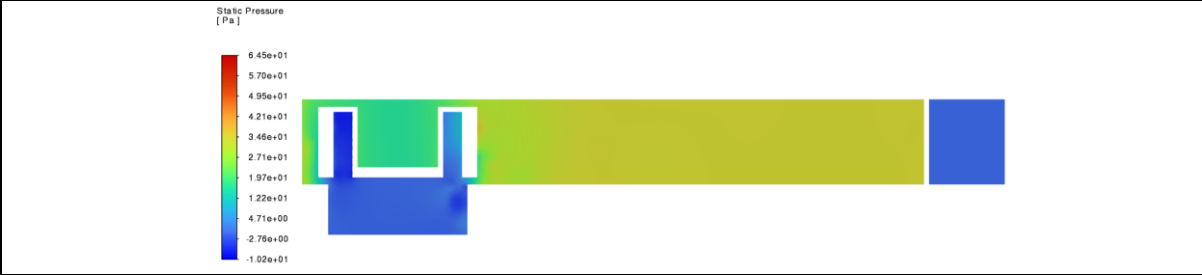


Figure 48. Static Pressure at Area (1%)

5.1.2 SimLab Model (Type 1)

Opening Rate	Pressure Difference (Pa)	Mass Flow Rate (kg/s)	Volumetric Flow Rate (m ³ /s)
100%	0	0.002094	0.0017393
80%	29.6547	0.001279	0.0010625
60%	37.9418	0.000999	0.0008301
40%	44.7894	0.000658	0.0005468
20%	49.9184	0.000317	0.0002630
0%	51.0264	0	0

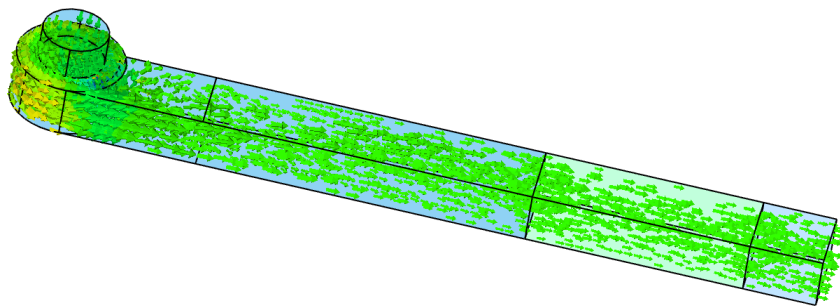


Figure 49. Static Pressure at Area (100%)

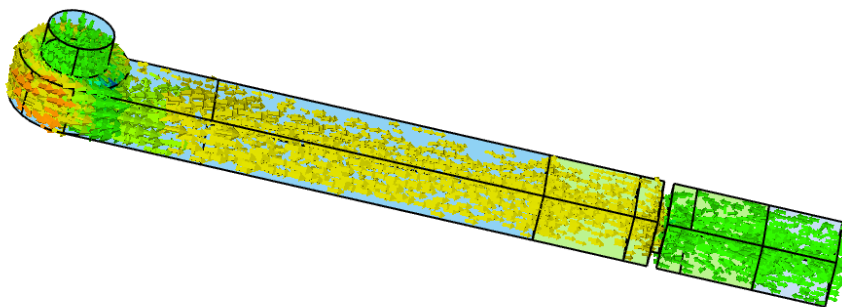


Figure 50. Static Pressure at Area (80%)

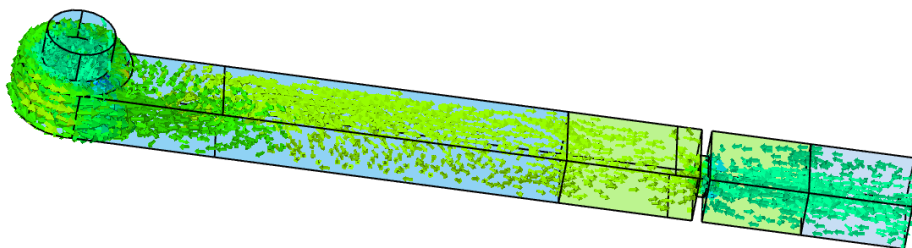


Figure 51. Static Pressure at Area (60%)

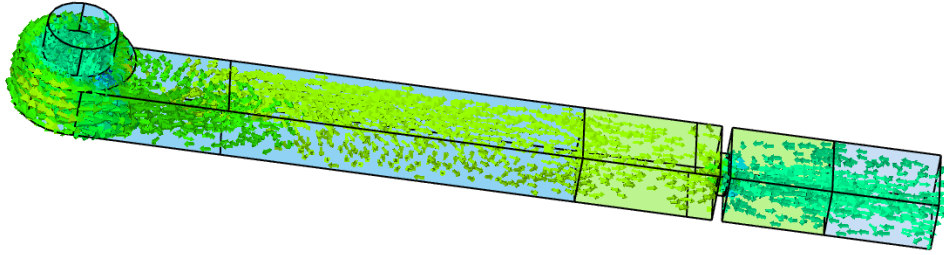


Figure 52. Static Pressure at Area (40%)

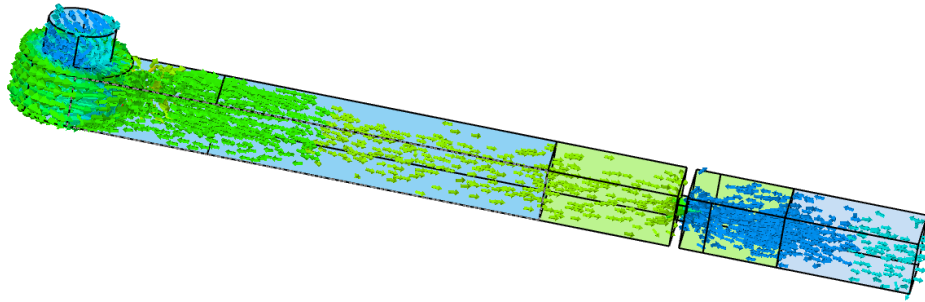


Figure 53. Static Pressure at Area (20%)

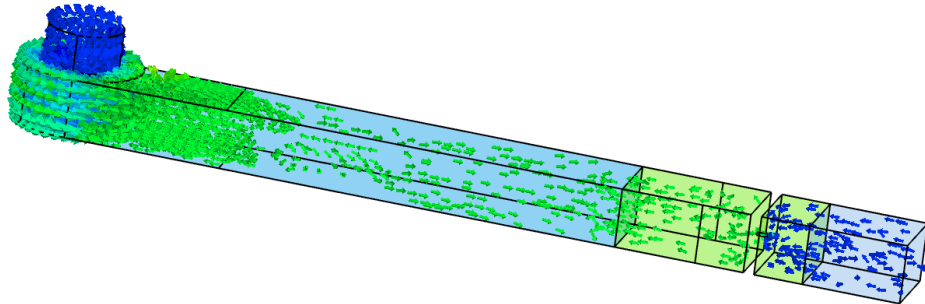
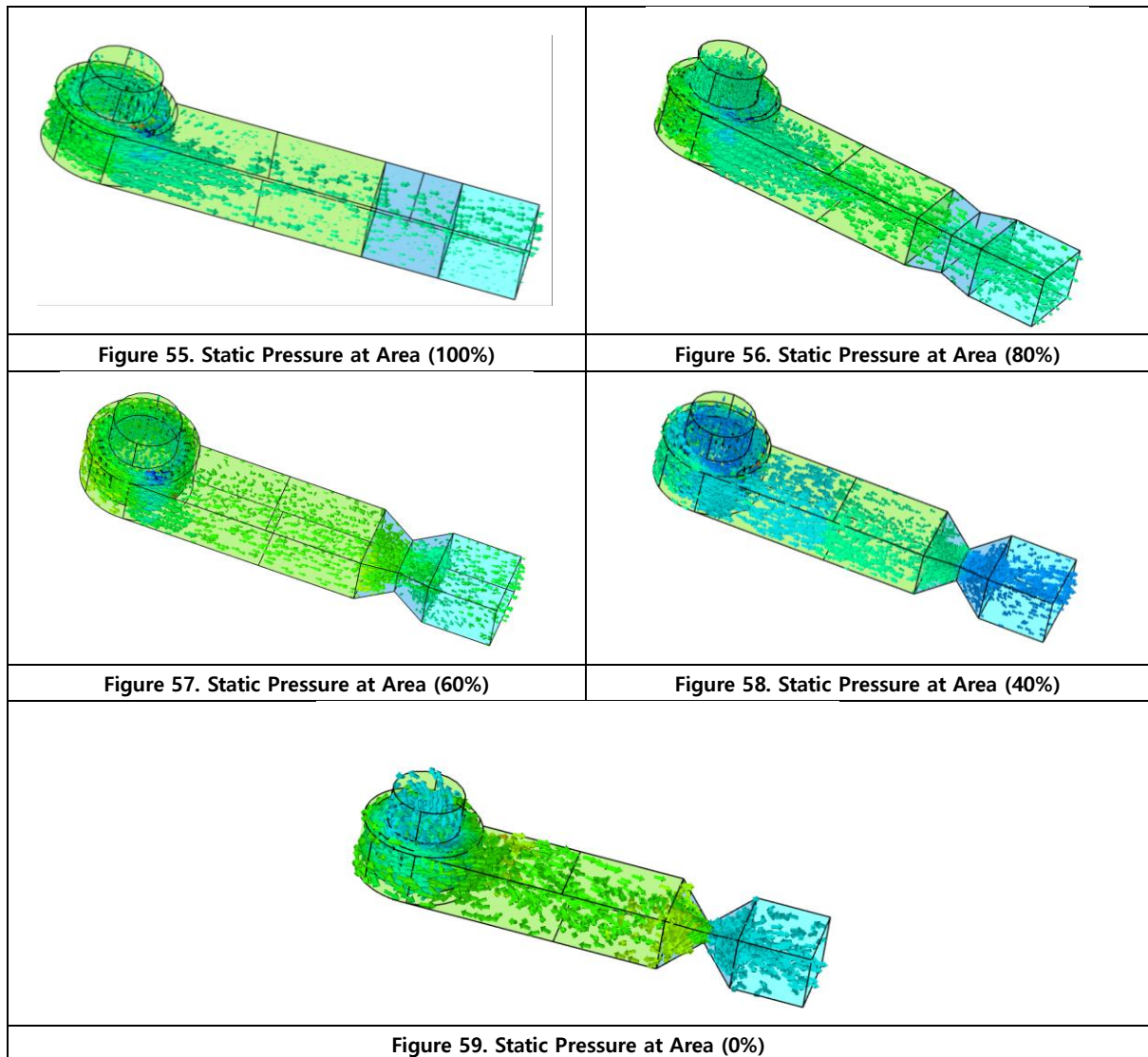


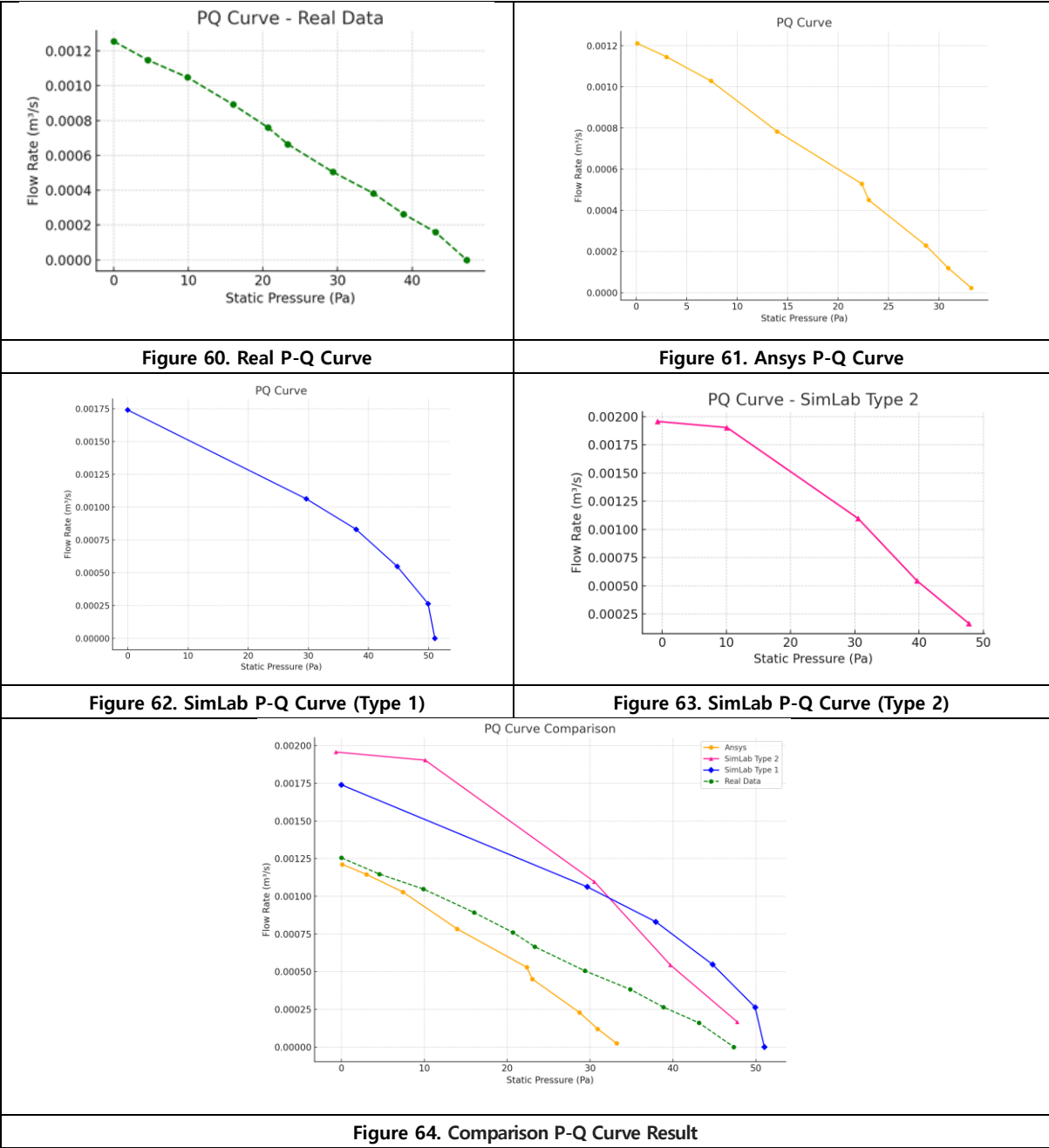
Figure 54. Static Pressure at Area (0%)

5.1.3 SimLab Model (Type 2)

Opening Rate	Pressure Difference (Pa)	Mass Flow Rate (kg/s)	Volumetric Flow Rate (m ³ /s)
100%	-0.67198	0.002398	0.001957
80%	10.10223	0.002331	0.001903
60%	30.52509	0.001342	0.001096
40%	39.68466	0.000667	0.000544
0%	47.75778	0.000203	0.000166



5.2 Comparison P-Q Curve Result



5.3 Comparison Between Simulation Results and Commercial Data Results

The Ansys model, which most closely resembled the actual geometry, produced results most similar to the real data.

Following that, SimLab (Type 1) yielded comparable outcomes. SimLab (Type 2) showed a generally decreasing trend consistent with a typical P-Q curve, but noticeable differences from the actual data were observed. This confirms that, in order to obtain reliable results, CAE analysis must be conducted under conditions that closely resemble the actual experiment.

6. Conclusion

6.1 Professional Ethical Issues, Responsibilities, and Attitudes in

Reporting CFD Results

CFD is utilized as a core tool in various engineering decision-making processes, such as product design, performance evaluation, and safety assessment. As such, its results are not merely technical data, but serve as critical grounds for actual policy decisions and directions in product development. Given the significant impact of these analytical results, accuracy, honesty, and transparency in reporting are essential, and engineers bear a great ethical responsibility in this regard.

1) Selective Interpretation of Results

The act of deliberately extracting only favorable simulation results while omitting unfavorable or unexpected outcomes constitutes selective interpretation. This can distort the overall understanding of performance or risk factors, potentially leading to serious errors in subsequent decision-making. All results must be presented in a balanced manner, and even outcomes that deviate from expectations should be objectively described with a review of their underlying causes.

2) Data Manipulation and Visual Distortion

This refers to cases where numerical data or graphs are manipulated, or visual elements (such as axis ranges, colors, units, etc.) are altered to intentionally distort the results when writing reports. A common issue includes compressing axes to exaggerate performance or selectively highlighting specific regions.

Such practices undermine trust and significantly increase the potential for misinterpretation.

3) Concealment of Uncertainty

CFD simulation results inherently contain various uncertainties due to factors such as model simplifications and mesh quality. Omitting or underestimating these margins of error or sensitivity analysis results in reports can lead to a false perception of the reliability of the analysis. Mesh independence checks, model validation outcomes, and similar evaluations must be clearly stated, and the limits of result reliability should be disclosed transparently.

4) Improper Use of Models

Using analysis models that do not align with the actual physical phenomena (e.g., inappropriate turbulence models, omission of viscosity analysis, etc.) can lead to incorrect conclusions if their limitations and assumptions are not clearly stated.

Since CFD models are idealized numerical methods, applying them without validating physical plausibility can be considered a serious ethical issue.

5) Improper Setting of Simulation Conditions

Intentionally using boundary conditions, initial conditions, or flow conditions that differ from reality to obtain favorable results, or excluding unfavorable conditions from the analysis, constitutes clear manipulation.

Setting excessively high inlet velocities or limiting the simulation domain to a restricted area reduces the representativeness of the results and can lead to design errors.

6) Violation of Copyright and Data Ownership

Using others' CFD results or models without proper citation, or utilizing such results without permission, constitutes copyright infringement.

In particular, when incorporating results from external companies or other researchers into internal reports or academic papers, it is essential to clearly indicate the source and obtain prior authorization.

7) Exaggeration of Performance and Potential for Misinterpretation

Adjusting simulation results or using overly optimistic language in reports or presentations to make performance appear better than it actually is can obscure accountability when issues arise later. Simulation outcomes must be presented as accurately as possible, including trends and limitations under various conditions. Excessive subjective interpretation by the analyst should be avoided.

These ethical issues are not mere mistakes; they are critical matters that can affect product safety and even human lives. Therefore, engineers conducting CFD analyses must possess not only the technical capability to perform simulations but also the responsibility to handle and report results with integrity. A professional attitude grounded in transparency and honesty is essential.

6.2 Time and Cost Advantages of CFD-Based Analysis Methods

1. Time Savings Compared to Physical Experiments

Traditional physical tests involve lengthy equipment setup, calibration, and repeated measurements, especially for complex geometries or extreme conditions. CFD enables rapid changes in boundary conditions, material properties, and geometry within a virtual environment, allowing automated execution of multiple scenarios once the mesh and model are established. This significantly shortens iteration cycles, accelerates design exploration (e.g., duct shapes or operating speeds), and helps detect flaws early, reducing the need for physical tests and improving development schedules.

2. Cost Reduction

Physical experiments incur high costs for prototypes, measurement equipment, facility operation, and external testing services. While CFD demands initial investments in software licenses and computing resources, it substantially lowers costs by reducing repeated prototype fabrication and enabling early detection of design inefficiencies. Flexible use of cloud or on-premises HPC further optimizes expenses during peak demand. Overall, CFD's operational costs often prove more economical than extensive experimental campaigns, especially in early design exploration.

3. Flexibility in Analyzing Variable Conditions

Unlike physical tests that require reconfiguration and safety checks for each scenario, CFD easily incorporates variations in inlet velocity, pressure, temperature, material properties, and geometry through scripting or parametric setups. This allows swift exploration of optimal operating points across diverse conditions and integration of sensitivity analyses in automated loops. In complex multiphysics evaluations, CFD simplifies repeated studies, broadens the design-search space, and enables early risk identification to guide efficient planning of any necessary physical tests.

4. Visualization and Quantitative Data Provision

CFD generates intuitive visuals—streamlines, vector fields, pressure and temperature contours—that clarify complex flow behaviors for both experts and non-specialists. It also delivers quantitative data at specified locations (velocity, pressure, shear stress) and time-dependent trends in transient studies, supporting performance prediction and safety assessments. Such outputs strengthen arguments in reports and presentations and provide a

basis for comparing against experimental results to assess simulation reliability. Thus, combined visual and numerical insights enhance transparency and trust throughout R&D.

5. Capability to Analyze Conditions Difficult for Experiments

CFD can safely model hazardous or impractical scenarios—high-temperature/pressure environments, toxic fluids, very low flow rates, or intricate internal passages—providing early risk mitigation and preliminary validation. It enables detailed analysis of flows in areas challenging to measure directly, improving design understanding and early issue detection. For new materials or technologies with uncertain properties, CFD estimates performance to prioritize experiments. As a result, CFD complements and extends physical testing, serving as a robust tool for safety assurance and design innovation

Reference

1. Jiang, T. (2021). CFD modelling and simulation of a centrifugal fan (Master's thesis). Czech Technical University in Prague, Faculty of Mechanical Engineering
2. Korean Agency for Technology and Standards. (2007). KS B 6311: Test and Inspection Methods for Blowers [Test and inspection methods for blowers]. Korean Standards Association.
3. Air Movement and Control Association International, & American Society of Heating, Refrigerating and Air-Conditioning Engineers. (2016). ANSI/AMCA Standard 210-16 / ANSI/ASHRAE Standard 51-16: Laboratory methods of testing fans for certified aerodynamic performance rating. AMCA International.
4. International Organization for Standardization. (2017). ISO 5801:2017 – Fans —Performance testing using standardized airways (3rd ed.). Geneva, Switzerland: ISO.
5. PTHAUS, "The Meaning of y^+ (y-plus) Value in CFD Analysis." [Online]. Available: <https://pthaus.tistory.com/m/28>. [Accessed: Jun. 6, 2025].
6. David, "What is the Fan Curve," Ecogate, Jun. 2, 2020. [Online]. Available: <https://www.ecogate.com/post/what-is-the-fan-curve>. [Accessed: Jun. 6, 2025].
7. Altair, "SL 2300 Centrifugal Blower – With a Moving Reference Frame," Wistia [Online Video]. Available: <https://altair-2.wistia.com/medias/hwpeba01q3>. [Accessed: Jun. 6, 2025].
8. Same Sky, "CBM-4020B-160-367 – 3D Model Resource," [Online]. Available: <https://www.sameskydevices.com/product/resource/3dmodel/cbm-4020b-160-367>. [Accessed: Jun. 6, 2025].
9. Same Sky, CBM-40B Series DC Blower Datasheet, Sep. 12, 2024. [Online]. Available: <https://www.sameskydevices.com/product/resource/3dmodel/cbm-4020b-160-367>. [Accessed: Jun. 6, 2025].
10. Irena Kirova, M.Sc., "CFD or Wind Tunnel? 6 Most Important Benefits of Digital Flow Simulation for Engineers", Dlubal, <https://www.dlubal.com/en/solutions/application-areas/cfd-or-wind-tunnel>, 2024.11.05

11. AFRY, "Computational Fluid Dynamics to predict hazards & increase protection in HSE engineering", <https://www.afry.com/en/insight/enhancing-safety-cfd-based-consequence-analysis>, 2024.10.12
12. Fortissimo, "HPC-Cloud-based simulation of sports-car aerodynamics", https://www.fortissimo-project.eu/en/success-stories/417/hpccloudbased-simulation-of-sportscar-aerodynamics?utm_source=chatgpt.com, [Accessed: Jun. 6, 2025].
13. Mohsen Seraj, "Accelerate CFD Simulation with Adaptive Mesh Refinement: Best Practices", OZEN, https://blog.ozeninc.com/resources/best-practice-for-adaptive-mesh-refinement-in-ansys-fluent?utm_source=chatgpt.com, 2024.11.15.
14. Lorsung, C., & Farimani, A. B. (2022, December 2). MeshDQN: A deep reinforcement learning framework for improving meshes in computational fluid dynamics (Cornell University). Carnegie Mellon University.
15. Bhoomi Gadhia, "Into the Omniverse: Computational Fluid Dynamics Simulation Finds Smoothest Flow With AI-Driven Digital Twins", NVIDIA, https://blogs.nvidia.com/blog/computational-fluid-dynamics-digital-twins/?utm_source=chatgpt.com, 2025.05.15.
16. Bismarck Martinez, "Better AI Could Mean Smooth Sailing in the World of Turbulence Modeling", Aerospace Engineering and Engineering Mechanics, https://www.ae.utexas.edu/news/better-ai-could-mean-smooth-sailing-in-the-world-of-turbulence-modeling?utm_source=chatgpt.com, 2024.12.16.
17. SIEMENS, "Siemens acquires Altair to create most complete AI-powered portfolio of industrial software", https://newsroom.sw.siemens.com/en-US/siemens-altair-engineering-closing/?utm_source=chatgpt.com, 2025.03.26
18. NVIDIA, "NVIDIA Announces Omniverse Real-Time Physics Digital Twins with Industry Software Leaders", https://investor.nvidia.com/news/press-release-details/2024/NVIDIA-Announces-Omniverse-Real-Time-Physics-Digital-TwinsWith-Industry-Software-Leaders/default.aspx?utm_source=chatgpt.com, 2024.11.18
19. Cadence, "Cadence Unveils Millennium Platform—Industry's First Accelerated Digital Twin Delivering Unprecedented Performance and Energy Efficiency", https://www.cadence.com/en_US/home/company/newsroom/press-releases/pr/2024/cadence-unveils-millennium-platformindustrys-first-accelerated.html?utm_source=chatgpt.com, 2024.02.01